



HAL
open science

Bunsen section thermodynamic model for hydrogen production by the sulfur-Iodine cycle

Mohamed Hadj-Kali, Vincent Gerbaud, Patrick Lovera, Olivier Baudouin, Pascal Floquet, Xavier Joulia, Jean-Marc Borgard, Philippe Carles

► **To cite this version:**

Mohamed Hadj-Kali, Vincent Gerbaud, Patrick Lovera, Olivier Baudouin, Pascal Floquet, et al.. Bunsen section thermodynamic model for hydrogen production by the sulfur-Iodine cycle. International Journal of Hydrogen Energy, 2009, 3 (16), pp.6625-6635. 10.1016/j.ijhydene.2009.06.022 . hal-03573174

HAL Id: hal-03573174

<https://hal.science/hal-03573174>

Submitted on 14 Feb 2022

HAL is a multi-disciplinary open access archive for the deposit and dissemination of scientific research documents, whether they are published or not. The documents may come from teaching and research institutions in France or abroad, or from public or private research centers.

L'archive ouverte pluridisciplinaire **HAL**, est destinée au dépôt et à la diffusion de documents scientifiques de niveau recherche, publiés ou non, émanant des établissements d'enseignement et de recherche français ou étrangers, des laboratoires publics ou privés.



Open Archive TOULOUSE Archive Ouverte (OATAO)

OATAO is an open access repository that collects the work of Toulouse researchers and makes it freely available over the web where possible.

This is an author-deposited version published in : <http://oatao.univ-toulouse.fr/>
Eprints ID : 3131

To link to this article : DOI:[10.1016/j.ijhydene.2009.06.022](https://doi.org/10.1016/j.ijhydene.2009.06.022)
URL : <http://dx.doi.org/10.1016/j.ijhydene.2009.06.022>

To cite this version :

Hadj-Kali, Mohamed and Gerbaud, Vincent and Lovera, Patrick and Baudouin, Olivier and Floquet, Pascal and Joulia, Xavier and Borgard, Jean-Marc and Carles, Philippe (2009) *Bunsen section thermodynamic model for hydrogen production by the sulfur-Iodine cycle*. International Journal of Hydrogen Energy, vol. 34 (n° 16). pp. 6625-6635. ISSN 0360-3199

BUNSEN SECTION THERMODYNAMIC MODEL FOR HYDROGEN PRODUCTION BY THE SULFUR - IODINE CYCLE

Published in Int. J. Hydrogen Energy, 34(16), 6625-6635, 2009

Bunsen section thermodynamic model for hydrogen production by the sulfur-
iodine cycle

Mohamed Kamel Hadj-Kali^{1,2}, Vincent Gerbaud^{1,2,*}, Patrick Lovera³, Olivier Baudouin⁴,
Pascal Floquet^{1,2}, Xavier Joulia^{1,2}, Jean-Marc Borgard³, Philippe Carles³

¹Université de Toulouse, INP-ENSIACET, UPS, LGC (Laboratoire de Génie Chimique), 118,
route de Narbonne F-31078 Toulouse Cedex 04 – France

²CNRS, LGC (Laboratoire de Génie Chimique), 5 rue Paulin Talabot, F-31106 Toulouse
Cedex 01 – France

³CEA, DEN, Physical Chemistry Department, F-91191 Gif-sur-Yvette, France.

⁴ ProSim, Stratège Bâtiment A, BP 27210, F-31672 Labège Cedex, France.

* corresponding author Vincent.Gerbaud@ensiacet.fr

Abstract

A model for the Bunsen section of the Sulfur – Iodine thermo-chemical cycle is proposed, where sulfur dioxide reacts with excess water and iodine to produce two demixing liquid aqueous phases (H_2SO_4 rich and HI rich) in equilibrium. Considering the mild temperature and pressure conditions, the UNIQUAC activity coefficient model combined with Engels' solvation model is used. The complete model is discussed, with HI solvation by water and by iodine as well as H_2SO_4 solvation by water, leading to a very high complexity with almost hundred parameters to be estimated from experimental data. Taking into account the water excess, a successful reduced model with only 15 parameters is proposed after defining new apparent species. Acids total dissociation and total H^+ solvation by water are the main assumptions. Results show a good agreement with published experimental data between 25 °C and 120 °C.

Keywords: Sulfur – Iodine cycle, Bunsen section, phase equilibrium modeling, liquid – liquid equilibrium

1. Introduction

Hydrogen is undeniably a very attractive energy carrier, superior to others for power generation, transportation and storage. Nowadays, fossil resources account for 95% of hydrogen production. However, given the prospect of an increasing energy demand, of a shortage of fossil resources and of greenhouse gases release limitation, water could be the only viable and long term candidate raw material for hydrogen production. Electrolysis and thermo-chemical cycles are the two leading processes for massive hydrogen production from water. In thermo-chemical cycles, water is decomposed into hydrogen and oxygen via chemical reactions using intermediate elements which are recycled. As the heat can be directly used, these cycles have the potential of a better efficiency than alkaline electrolysis. For massive hydrogen production, the required energy can be provided either by nuclear energy, by solar energy or by hybrid solutions including both.

Please, insert Figure 1 here

Among hundreds of possible cycles, the Sulfur – Iodine (S-I) cycle is a promising one [1] in combination with high temperature heat, having no solid phase under the process operating conditions. The S-I thermo-chemical cycle, depicted in figure 1, is divided into three sections, namely: (I) the Bunsen section, where water H_2O reacts with iodine I_2 and sulfur dioxide SO_2 to produce, by using a specific stoichiometry, two immiscible liquid aqueous phases: one phase containing mainly sulfuric acid H_2SO_4 and the other phase containing hydroiodic acid (hydrogen iodide) HI and iodine I_2 (known as the HI_x phase); (II) the sulfuric acid and (III) the hydrogen iodide concentration and decomposition sections, where intermediate products break down upon heating, releasing hydrogen and oxygen. Water, iodine and sulfur dioxide are recycled in the system [2].

In 2005, Mathias quoted the thermodynamic systems occurring in the Bunsen section and the HI_x section among current challenges for applied thermodynamics [3]. He wrote: “...*The sulfuric acid decomposition section of ...[the S-I]... process can be simulated accurately, but other sections (acid generation and hydrogen iodide decomposition) illustrate the difficulty of modeling phase behavior, particularly liquid-phase immiscibility, in complex electrolyte systems.*” Acid generation refers to the Bunsen section.

We have recently proposed a new approach to model the HI_x section [4]: the Peng Robinson equation of state (EoS) approach is supplemented with the MHV2 complex mixing rule that incorporates an Excess Gibbs energy model (G^{EX}) to handle the strong non ideal behavior of the HI_x system. UNIQUAC G^{EX} model is combined with solvation of hydrogen iodide HI by water H_2O according to Engel’s solvation model. In the HI_x section, the resulting EoS/ G^{EX} model is able to describe with accuracy, by using a single set of parameters, all literature vapor – liquid, liquid – liquid, vapor – liquid – liquid and solid – liquid equilibrium data for the HI_x ternary system and the three binary subsystems. Compared to other models for the HI_x system based on an electrolyte model [5-7], the homogeneous EoS/ G^{EX} approach of Hadj-Kali *et al.* [4] has two major interests: first, it is theoretically compatible with calculations above HI critical temperature, that is likely to occur if a reactive distillation process is chosen for the HI_x section [8-10]. Second, using Engel’s solvation model for the solvation of HI by H_2O , like Neumann’s model [11,12], it is based on a symmetric convention in which the same reference state is supposed for all species, enabling to readily explore equilibrium properties for any composition. Because of a lack of experimental data under the HI_x system conditions, HI dissociation reaction, producing H_2 and I_2 was not considered [4]. Polyiodide formation in aqueous solution [13-15] was not explicitly considered for the HI_x section but is likely to occur in the Bunsen section, because the milder temperature favors polyiodide formation.

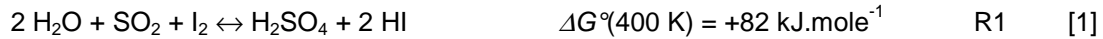
In continuation of the modeling work of the HI_x section, the present paper focuses on the thermodynamic modeling of the Bunsen section. At low pressures, a homogeneous EoS/ G^{EX} approach is not mandatory to model the liquid – liquid equilibrium occurring. We then inspire from the G^{EX} part of the model of Hadj-Kali *et al.* [4] by combining the UNIQUAC model with Engel’s solvation.

2. Background

2.1. Bunsen section reactions

2.1.1. Bunsen main reaction

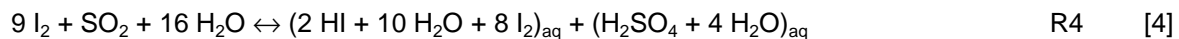
Bunsen main reaction is the following:



With ΔG° being the standard Gibbs free energy. The positive value of $\Delta G^\circ(400 \text{ K})$ implies an extremely small equilibrium constant $K(400 \text{ K})=1.96 \cdot 10^{-11}$. Thus the formation of the acids H_2SO_4 and HI is not favored unless one of them at least is removed from the reactor. However, according to Le Châtelier's principle, any excess of reactant will be consumed and produce the acids. Indeed iodine in excess favors the production of the acids and the spontaneous demixion into two aqueous solutions, a light one rich in H_2SO_4 (SA phase) and a heavy one rich in HI (HI_x phase). According to Elder *et al.* [16], the two aqueous phases demixion arises from the formation of polyiodide ions as iodine ions in the HI phase are solvated by molecular iodine. Besides, water excess enables to dilute both acids with a negative standard Gibbs energy [16]:



Therefore, the overall reaction is (R1) + (R2) + (R3) and General Atomics [17] proposed the typical equation for the Bunsen process:



This reaction strongly favors the production of the aqueous acid phases as its standard Gibbs energy equals $\Delta G^\circ(400 \text{ K}) = -88 \text{ kJ.mole}^{-1}$, leading to an equilibrium constant value $K(400 \text{ K}) = 3.1 \cdot 10^{+11}$.

Finally, Kracek [18] observed that below 493 K, $\text{H}_2\text{O} - \text{I}_2$ binary mixture has a very large immiscibility gap between approximately $n\text{H}_2\text{O}/n\text{I}_2 \in \{0.03; 99\}$, encompassing both water – iodine molar ratio in reaction R1 ($n\text{H}_2\text{O}/n\text{I}_2=2$) or R4 ($n\text{H}_2\text{O}/n\text{I}_2=1.78$ for the reactants, $n\text{H}_2\text{O}/n\text{I}_2=1.75$ for the products) and thus likely explaining why demixion occurs.

2.1.2. Bunsen section side reactions

Side reactions occur in the Bunsen section to produce sulfur S and hydrogen sulfide H_2S [19]:



Sakurai *et al.* [19] studied in HI, H_2SO_4 and I_2 solutions the concentration and temperature conditions under which those side reactions occur: reaction R6 is favored between 295 K and 368 K over reaction R5, the opposite under low iodine excess; both equations are overall enhanced by a higher temperature, higher acid concentrations and low iodine excess. They suggest that operating at 368 K requires to control iodine concentration so that poly hydroiodic (HI_x) acids is above $x = 4.41$ to avoid side-reactions and below $x = 11.99$ to prevent iodine crystallization.

2.1.3. Polyiodides formation

The solvation power of iodine is well known and quite similar to water solvation. Palmer and Lietzke [13] have studied the kinetics and equilibria of iodine hydrolysis. They postulated the existence of I^- , I_3^- , I_2O^- , OI^- ions, giving for each one a mathematical expression of the equilibrium constant, while discarding I_5^- and I_6^{2-} ions regarding their low iodine concentration during the experiments. The following reaction illustrates the polyiodides formation:



with

$$T \cdot \ln K = 3727.86 - 11.6326 \cdot T + 0.019221 \cdot T^2 \quad [8]$$

Calabrese and Khan [15] also identified I_3^- and several polyiodide ions I_{2x}H^+ (with $x = 2, 3$, etc.) in aqueous solutions of KI where iodine is introduced. Again, they discard I_5^- and I_7^- ions regarding the

low iodine content introduced. The equilibrium constant expression (equation 8) suggests that I_3^- is favored at the temperature expected for the Bunsen section.

2.2. Liquid – liquid equilibrium experimental data

Two experimental approaches are considered. The first mixes Bunsen reaction's three reactants (SO_2 , I_2 and H_2O) at various temperatures and explores in so-called 1/m/n data points the impact of m or n molecules of iodine or water reacting with SO_2 . General Atomic typical stoichiometry of reaction R4 corresponds to a 1/9/16 data point.

The second approach mixes the four reaction products, H_2SO_4 , HI, I_2 and H_2O at various temperatures and explores in so-called 1/a/b/c data points the impact of HI (a), I_2 (b) and H_2O (c) mole number in contact with one sulfuric acid mole. General Atomic typical stoichiometry of reaction R4 corresponds to a 1/2/8/14 data point. Usually iodine content has a lower limit to ensure liquid – liquid phase split and an upper one to avoid iodine precipitation.

Sakurai *et al.* [20,21] have analysed the influence of temperature and iodine for various initial mixtures $H_2SO_4/HI/H_2O = 0.048/0.070/0.882$ (at 273, 301, 313, 333, 353 and 368 K), $H_2SO_4/HI/H_2O = 0.058/0.085/0.857$ (at 313 K), $H_2SO_4/HI/H_2O = 0.069/0.049/0.882$ (at 313 K). Among their conclusions, they noticed that the impurity content in each phase (i.e. H_2SO_4 in HI_x phase and I_2 together with HI in SA phase) decreases as the iodine content increases. They also noticed that under iodine saturation conditions, separation at 368 K enables to reduce by 25% impurities in the HI_x phase and by 20% in the SA phase. Experimental data accuracy is not known.

Kang *et al.* [22] carried out a large set of experiments between 298 K and 393 K for 1/2/0.5~8/14~20 data points. The lowest impurities are achieved at 353 K with the highest iodine content. They also notice that excess water has more affinity with the HI_x phase than with the SA phase, but that this affinity decreases with temperature and increases with iodine molar fraction.

Giaconia *et al.* [23] published 1/2/4~16 /11.2~15.8 data points from 353 K to 393 K. They concluded that the temperature and iodine content did not affect much the HI and H_2SO_4 split among the HI_x phase and the SA phase. They also noticed that high iodine content reduced impurities in both phases and that excess water goes into the SA rich phase. Accuracy is claimed to be 0.002 molar fraction for HI and I_2 in the SA phase and 0.01 molar fraction for all other species in the SA and HI_x phase.

Lee *et al.* [24] have reviewed the aforementioned literature Bunsen section liquid – liquid equilibrium experimental data in terms of 1/a/b/c data points, including other Korean data points from a Master's thesis (see [24]). They have combined them in a database of 69 data points to highlight the temperature, HI content and excess iodine and water in the feed. This database is consistent despite the absence of accuracy data and is used as a reference in the present work.

2.3. Bunsen section thermodynamic and former models

2.3.1. Liquid – Liquid equilibrium

Liquid – liquid equilibrium are computed from the usual thermodynamic condition, activities equality:

$$a_i(T, \mathbf{x}) = a_i(T, \mathbf{x}') \quad \text{or} \quad \gamma_i(T, \mathbf{x}) \cdot x_i = \gamma_i(T, \mathbf{x}') \cdot x'_i \quad [9]$$

It then requires an excess Gibbs energy model to compute the activities a_i or the activity coefficients γ_i .

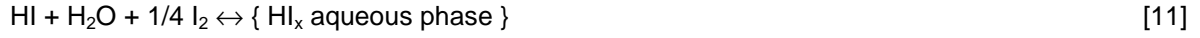
2.3.2. Non ideal solution behavior: former thermodynamic models

Bunsen section compounds form a strongly nonideal mixture. Occurrence of strong acids like HI and H_2SO_4 in aqueous solutions hints at the occurrence of electrolytes, well known to interact over long range. The nonideal behavior could be handled using an excess Gibbs energy model.

Literature models on the Bunsen section are scarce and not fully satisfying.

Davis and Conger [25] proposed an electrolytic activity coefficient model based on a Pitzer-Debye-Hückel approach. They describe the sulfuric and hydroiodic acid phases by the dissociation equations relative to H_2SO_4 , SO_2 , and water, and to HI, SO_2 and water respectively. Therefore, they imply that H_2SO_4 is found only in the SA phase and HI only in the HI_x phase. They validate the model on a single experimental point with initial $nH_2O/nI_2 = 2.0713$ at 368 K. Their results underestimate the water quantity in the SA phase and thus overestimate it in the HI_x phase.

Mathias [26] used the electrolyte-NRTL model developed by Chen *et al.* [27,28] that combines the Pitzer-Debye-Hückel model [29] for long-range ion-ion electrostatic interactions with the NRTL theory [30] for short-range energetic interactions among the species in electrolyte solutions. The reactions considered are:



Mathias indicates that iodine and HI form the complex HI_x in aqueous solutions, of which exact composition "x" should be determined to best describe experimental data.

Recently, O'Connell [31] hinted at a possible improvement of Mathias' approach by considering the two reactions:



No consistent results are provided though.

Those electrolyte models are based on an asymmetric convention for the electrolyte and the solvent which does not allow their application over the entire composition range [32]. Chen's electrolyte-NRTL model claims accurate prediction of activity coefficient up to 16 mol/kg of solvent for strong acid electrolytes like HCl or H_2SO_4 [33].

3. Bunsen section new thermodynamic model

We propose to combine the UNIQUAC model for non ideal interactions phenomena with Engel's solvation model for long range electrolytic interaction phenomena. A similar approach was used successfully alone and into the MHV2 complex mixing rule applied to the Peng Robinson equation of state to model the HI_x section thermodynamics [4].

However, application to the Bunsen section phenomena rapidly leads to an unsolvable complexity, which hinted us at devising a simplified representation of the phenomena.

3.1. Thermodynamic model

3.1.1. Non ideal interaction model: UNIQUAC

The local composition model UNIQUAC is based on a symmetric convention for all species. UNIQUAC sums a combinatorial term accounting for the entropic contribution and a residual term accounting for intermolecular interactions, responsible for the mixing enthalpy [34].

$$\frac{G^{Ex}}{RT} = \left(\frac{G^{Ex}}{RT} \right)_{\text{combinatorial}} + \left(\frac{G^{Ex}}{RT} \right)_{\text{residual}} = f_{\text{combinatorial}}(\mathbf{x}, r, q) + f_{\text{residual}}(\mathbf{x}, q', A_{ij}, A_{ji}) \quad [14]$$

The activity coefficient expression is:

$$\ln \gamma_i = \left(\ln \frac{\phi_i}{x_i} + \frac{z}{2} q_i \ln \frac{\theta_i}{\phi_i} + l_i - \frac{\phi_i}{x_i} \sum_{j=1}^n x_j l_j \right) + \left(q'_i - q'_i \ln \left(\sum_{j=1}^n \theta_j \tau_{ji} \right) - q'_i \sum_{j=1}^n \frac{\theta'_j \tau_{ij}}{\sum_{k=1}^n \theta'_k \tau_{kj}} \right) \quad [15]$$

$$\text{with: } \tau_{ij} = \exp\left(-\frac{A_{ij}}{RT}\right), \tau_{ii} = \tau_{jj} = 1, l_i = \frac{z}{2}(r_i - q_i) - (r_i - 1), z = 10$$

$$\phi_i = \frac{x_i r_i}{\sum_j x_j r_j} \quad \theta_i = \frac{x_i q_i}{\sum_j x_j q_j} \quad \theta'_i = \frac{x_i q'_i}{\sum_j x_j q'_j}$$

Binary interaction parameters A_{ij} and A_{ji} (in cal/mol) are estimated from experimental data, considering a temperature linear dependency:

$$A_{ij} = A_{ij}^0 + A_{ij}^T T \quad [16]$$

Parameters r_i , q_i and q_i' are molecular constants that can be estimated for any new species, like solvation complexes, using the group contribution method of Bondi [35], as suggested by UNIQUAC author's [34,36].

3.1.2. Long range electrolytic interactions: Engels' solvation model

An alternative model for electrolytes is provided by Engels solvation model, based on the concept that ions exist in solution only within a stable solvent cloud [37]. The new molecule clusters called "complexes" C are made by the reaction of m solvent molecules S with one electrolyte E molecule according to the expression:



Where ν is the number of dissociation products of one electrolyte molecule; x_i is the molar fraction of the species i and a_i , γ_i their activity and activity coefficient respectively. K is the solvation constant with a temperature dependency like:

$$K = \exp(A_K + B_K / T) \quad [18]$$

where A_K and B_K are the solvation constant parameters.

This model uses a symmetric convention for both the electrolyte and the solvent, removing any limitation over the composition range. Under dilute electrolyte conditions, the excess of solvent favors the complete dissociation and solvation of the electrolyte. Near pure electrolyte, lack of solvent leaves the electrolyte undissociated. For $H_2O - HI$ mixtures, this is consistent with solid – liquid equilibrium data [38] showing a decrease in the hydration number in solid HI, nH_2O as water composition decreases.

Equation (17) results from the strict thermodynamic description of an electrolyte dissociation followed by solvation of the cation. For example, for $H_2O - HI$, we write:



The equilibrium constant of equations (17) and (20) are equivalent with a complex $2C$ that would be like $\{[H_3O^+, (m-1)H_2O]; I^-\}$. Writing of H_3O^+ is based on hydronium ion evidence in aqueous solutions, with a hydration number that may vary upon conditions [39].

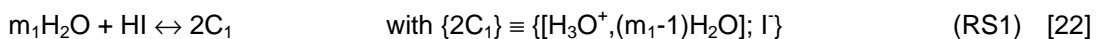
Engels' model was first used successfully by its author with the Wilson activity coefficient model [37] to describe the vapor – liquid phase equilibrium of the binary mixture $H_2O - HI$. It was also successfully used in several thermodynamic approaches of the HI_x section in the Sulfur – Iodine thermochemical cycle, by Neumann [11], Yoon *et al.* [12] and Hadj-Kali *et al.* [4] to account for HI solvation by water.

3.2. Bunsen section complete model

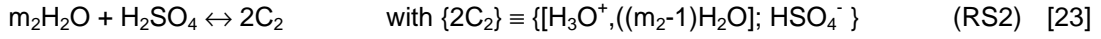
One of the challenges of the Bunsen section is to investigate how much excess water and iodine can be reduced so as to limit the recycle flowrates, without impeding the two acid phase production by reaction R1 or R4 and maintaining side reactions R5 and R6 under control. However, based on the information available in Lee's data compilation, we restrict ourselves to consider the Bunsen forward reaction, discarding SO_2 , S or H_2S species.

At first the UNIQUAC + Engels solvation model can handle the following phenomena:

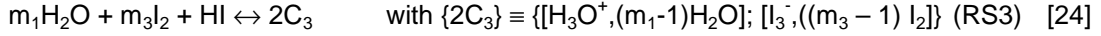
1. Liquid – liquid equilibrium between the SA phase and the HI_x phase.
2. Solvation of HI by H_2O (HI_x phase):



3. Solvation of first acidity of H_2SO_4 by H_2O (SA phase):



4. Solvation of HI by I₂ in the presence of water (HI_x phase):



Therefore, there are n=7 true species: I₂, HI, H₂O, H₂SO₄, C1, C2 and C3 with 93 parameters requiring estimation: 84 parameters, A_{ij}^0 , A_{ji}^0 , A_{ij}^T and A_{ji}^T for the calculation of the n(n-1) binary interactions A_{ij} et A_{ji} from equation (16); 2 parameters A_K and B_K for each three solvation constant and, finally, three solvation numbers, m_1 , m_2 , m_3 .

3.3. Bunsen section simplified representation

3.3.1. Measured, apparent and true species

The analysis of literature experimental data [19,21,23,24] shows that the measured molar ratio nH₂O/nHI and nH₂O/nH₂SO₄ is always greater than 3 in the initial composition or in the two equilibrium SA and HI_x aqueous phases composition. We take advantage of the water excess in the following hypotheses.

a. Hypothesis of acid total dissociation in excess water

Considering the HI dissociation constant in aqueous solution ($pK_a = -\log_{10} K_a = -10$ at 298K), we postulate that HI is fully dissociated. The same is assumed for the first acidity of H₂SO₄ ($pK_{a1} = -3$ at 298K):



The second acidity ($pK_{a2} = 1.99$ at 298K) is neglected.

b. Hypothesis of H⁺ ion solvation by three water molecules

All H⁺ ions are supposed to be solvated by three H₂O molecules, independently whether they come from HI or H₂SO₄ total dissociation ($m_1=m_2=3$ in equation (21) and (22)).

Those hypotheses a and b enable to substitute the measured species HI and H₂SO₄ by two apparent species, that we write [H₂SO₄,3H₂O] and [HI,3H₂O]. These apparent species correspond to the complexes $\{[\text{H}_3\text{O}^+, (m_2-1)\text{H}_2\text{O}]; \text{HSO}_4^-\}$ and $\{[\text{H}_3\text{O}^+, (m_1-1)\text{H}_2\text{O}]; \text{I}^-\}$.

Molar fractions of apparent species are computed from mass balances, accounting for the fact that apparent, or free, water now equals to the measured water minus the water used for the hydration of HI and H₂SO₄:

c. Hypothesis of hydrated HI acid solvation by iodine

To cope with the occurrence of polyiodides $[\text{I}^-, m_3\text{I}_2]$ in aqueous solution [13,14,15], each hydrated complex [HI, 3H₂O] is solvated by m₃ moles of iodine in excess following Engels' solvation model:



Furthermore, we postulate that $m_3 = 1$. So, $\{2\text{C}_3\}$ is also equivalent to $\{[\text{H}_3\text{O}^+, 2\text{H}_2\text{O}]; \text{I}_3^-\}$.

Together, these hypotheses lead to define four apparent species, I₂, free H₂O, [HI,3H₂O] and [H₂SO₄,3H₂O], and five true species when the $\{2\text{C}_3\}$ species is added. With five species, the number of parameters to identify reduces from 84 binary parameters to 40 and from 9 solvation parameters to 2. True species molar fractions are computed from mass balances and the solvation equilibrium equation (26).

In spite of these first level hypotheses, the total number of parameters of this simplified model, equal to 42, remains too much in front of the available experimental data. It is why a second level set of hypothesis must be formulated.

3.3.2. True species interaction matrix

We further postulate that [H₂SO₄,3H₂O] hydrated complex interacts like water with other species. Indeed, modeling of H₂O – H₂SO₄ binary mixtures vapor – liquid equilibrium using Engels' proposal

[37] shows that the interaction between water and the $\{2C_2\}$ solvation complex of H_2SO_4 by H_2O (see equation (23)) is negligible. By doing so, we consider that the chemical theory alone allow to represent the non ideal behavior of the solution.

Finally, we postulate that the new solvation complex $\{2C_3\}$ of $[HI,3H_2O]$ by I_2 behaves like I_2 and that their binary interaction is null.

The true species binary interaction parameter matrix becomes:

Please, insert Table 1 here

The number of binary parameters, A_{ij}^0 , A_{ji}^0 , A_{ij}^T and A_{ji}^T , reduces to 12 plus the 2 parameters A_K and B_K of the $\{C_3\}$ solvation constant. The solvation number m_3 is set to unity.

Interactions between H_2O and I_2 are initialised on the basis of liquid – liquid equilibrium data of Kracek [18] as done in a previous study [4].

The new species $[HI,3H_2O]$, $[H_2SO_4,3H_2O]$ and $\{2C_3\} \equiv \{[H_3O^+,2H_2O]; I_3^-\}$ are created in Simulis[®] Thermodynamics thermophysical properties calculation server [40] and their UNIQUAC parameters r_i , and q_i estimated according to Bondi's group contribution method [35].

4. Results

4.1. Data analysis

- The model parameters are estimated on the basis of the 45 of the 50 Korean points (K01 to K50) among the 69 $H_2SO_4/HI/I_2/H_2O$ data points combined by Lee *et al.* [24] covering temperatures from 298.15 K to 393.15 K. Lee *et al.* reported Giaconia and coworker's "point entry 5" [23] at a temperature of 368.5K instead of 393.5K. We corrected Lee's G06 accordingly. The remaining points from Giaconia (G01 to G10) and from Sakurai (S01 to S09) are used for validation only.
- Among the 69 experimental data points, 67 have enough water, globally and in both acid phases to ensure that apparent species $[H_2SO_4,3H_2O]$, $[HI,3H_2O]$, I_2 , H_2O molar fractions are physically coherent, that means positive. Indeed, experimental points G04 and G06 lack water in the HI_x phase to hydrate HI and H_2SO_4 with 3 H_2O in this phase. However, the water missing is very small and for these points the free water molar fraction in the HI_x phase is considered null for the purpose of calculating apparent species molar fraction.
- Experimental points G02 and G05 contain exactly enough water in the HI_x phase to hydrate HI and H_2SO_4 with 3 H_2O in this phase. The free water molar fraction is therefore null.
- Experimental points K19 and K38 show a suspiciously low H_2SO_4 molar fraction in the HI_x phase (0.003 and 0.008), compared to surrounding measures at the same temperature all at least twice greater.
- Experimental points K29, K40, K41, K42, K47, K48, K49, K50 of Lee *et al.* [24] show a zero molar fraction for impurity I_2 in the SA phase at temperature of 373.15K and 393.15K. Experimental points S09, G02, G05, G10 of Sakurai and Giaconia are alike.
- Molar fraction data show that in phase SA, I_2 and HI are impurities whereas H_2O and H_2SO_4 are the main species. In phase HI_x , H_2SO_4 is the impurity whereas H_2O , I_2 , and HI are the main species.
- Points K09, K14, K35, K36, K43 are the only points with a molar ratio $n_{I_2}/n_{H_2SO_4}$ lower than unity. They are excluded from the parameter estimation procedure.

4.2. Parameter estimation criterion

We use a relative least square criterion to enhance the weight of impurities molar fractions in the estimation procedures. The null molar fraction values are included in the criterion calculation by dividing the absolute error ($x^{exp} - x^{calc}$) by 0.001.

$$Criterion = \frac{1}{N'} \sum_{\varphi=1}^{HI_x, SA \text{ phases}} \left(\sum_{i=1}^{\text{apparent species}} \left(\sum_{j=1}^N \left(\frac{x_{i,j,\varphi}^{exp} - x_{i,j,\varphi}^{calc}}{x_{i,j,\varphi}^{exp}} \right)^2 \right) \right) \quad [26]$$

N is the number of points in each phase and N' is the total number of points.

4.3. Parameter set

Table 2 displays the binary interaction parameters for the true species and the parameters of the solvation constant of the Bunsen section simplified model.

Please, insert Table 2 here

Evidently, there is a strong correlation between the I_2 - $[HI, 3H_2O]$ binary parameters and the $[HI, 3H_2O]$ by I_2 solvation constant parameters. They are both used to balance the species repartition between iodine, hydrogen iodide (through $[HI, 3H_2O]$) and polyiodides (through the complex $\{2C_3\}$) in the mixtures. Solvation belongs to a chemical modelling approach; binary interaction parameters rather belong to a physical modelling approach. We experienced that both approaches are needed for the Bunsen section mixtures.

4.4. Discussion

Table 3 reports the mean and median relative errors on the experimentally measured molar fractions for all species, for all impurity species in both phases and for the main species in both phases. The values are also displayed for each of the six temperatures spanned by the Korean data used for the estimation of the parameters displayed in Table 2. Data of Sakurai *et al.* [20,21] and Giaconia *et al.* [23] are not used in the parameter estimation procedure but as validation of the model through their recording in Lee's table [24]. The median is also displayed, as being less influenced by extreme values.

Apparent species error values that were used in the procedure are not directly meaningful with respect to the experimentally measured data. Thus, they are not reported but can be obtained from the authors upon request.

Please, insert Table 3 here

4.4.1. Liquid – Liquid phase splitting

First, regarding liquid – liquid phase splitting, the 45 data points taken in the parameter estimation procedure demix according to the model's predictions. Sakurai's {S01-S09} points and Giaconia's {G01-G10} points also demix. The 5 points with $n_{I_2}/n_{H_2SO_4} < 1$ {K09; K14; K24; K35-K36; K43} do not demix, another reason for which we excluded them from the procedure. Kang *et al.* [22] also published four points where they reported no demixion. The model predicts correctly Kang's observations.

4.4.2. Deviation of the model from Lee's data points

Regarding the parameter estimation on Lee's data points, table 3 shows that the relative error is quite small for the main species, either the mean one equal to 5.8% or the median one to 2.9%. It is greater for the so-called impurity species, with the mean one equals to 27.5 % and the median one to 29.5%. This is due to the fact that relative errors are always large for small experimental molar fractions as those of impurities. Overall, for all species, the mean relative error (17.1%) and the median one (5.4%) are quite reasonable. Besides, according to table 3, there are no significant differences between the various temperature sets, hinting at a reasonable temperature dependency of the parameters.

Table 4 reports the median, mean and maximum relative errors for each experimentally measured species in each phase.

Please, insert Table 4 here

A closer look at each species (table 4) shows that in each phase the errors related to the main species are quite low, the largest being observed for H_2SO_4 in the SA phase. For the impurity species, table 4 shows that I_2 in the SA phase bears the greatest relative errors, being also the smallest impurity molar fraction.

Mean and median are alike, indicating no significantly large error, as it is confirmed by the moderate maximum error values.

The two suspicious H_2SO_4 molar fractions in the HI_x phase (K19 and K38 points) that are 0.0030 and 0.0080 molar fractions are computed as 0.0087 and 0.0104 respectively, larger values, in better accordance regarding the surrounding data points.

Experimental and calculated data values are displayed for the impurities and main component in the H_2SO_4 -rich phase and in the in the HI -rich phase. K09, K14, K35, K36, K43 data points are excluded for the reasons explained before. +10% and -10% error lines are displayed for indication. Figure 2 concerns 25°C and 40°C temperatures; Figure 3 concerns 60°C and 80°C temperatures; Figure 2 concerns 100°C and 120°C temperatures.

Please, insert Figure 2 here

First, we notice that in the H_2SO_4 -rich phase the model underestimate the molar fractions of the impurities HI and I_2 at 25°C and I_2 at 40°C. Other molar fractions are reasonably well predicted, in particular the H_2SO_4 impurity in the HI -rich phase. We do not understand why the underestimation does not concern HI at 40°C except that, if we assume that the model is correct, it may hint at some systematic deviation of the experimental data at 25°C (no information about the accuracy was given in [24]).

Please, insert Figure 3 here

At 60 and 80°C, there is still a systematic underestimation of I_2 in the H_2SO_4 -rich phase. For the other molar fractions, in particular for the other impurities in both phases, a scattering of the errors is observed. That could also indicate a scattering of the experimental data and hint at the experimental accuracy of these measurements.

Please, insert Figure 4 here

At 100°C and 120°C, I_2 is again underestimated in the H_2SO_4 -rich phase.

Overall, water is well predicted in the H_2SO_4 -rich phase, which suggests the pertinence of the hypothesis the $\text{H}_2\text{O} - \text{H}_2\text{SO}_4$ mixtures (complete dissociation of the first acidity, hydration of the hydronium ion into $\text{H}_2\text{SO}_4 \cdot 3\text{H}_2\text{O}$ and no interaction between water and $\text{H}_2\text{SO}_4 \cdot 3\text{H}_2\text{O}$). The same holds for the water in the HI -rich phase.

4.4.3. Validation on Sakurai's and Giaconia's data points.

Regarding the data points of Sakurai (S01 to S09 in [24]) and Giaconia (G01 to G10 in [24]), the prediction bears the same remarks than for the Korean data but the errors are generally greater (see Table 3).

For the impurity H_2SO_4 in the HI rich phase in Giaconia's data points, the median relative error is much smaller than the mean relative error, indicating that unusually large errors, as confirmed by the very large maximum error of 494% (see Table 4). It corresponds to data point S08 where the H_2SO_4 molar fraction in the HI rich phase is the smallest (0.002) and of the order of magnitude of the experimental error reported by Giaconia *et al.* [23].

Experimental and calculated data values are displayed in Figure 5 for the impurities and main component in the H_2SO_4 -rich phase and in the in the HI -rich phase. +10% and -10% error lines are displayed for indication.

Please, insert Figure 5 here

They show a trend of the model to underestimate the impurities I_2 and HI in the H_2SO_4 -rich phase for sakurai's datapoint and to overestimate the impurity H_2SO_4 in the HI -rich phase for Giaconia's points.

Overall, despite its achievements in representing the literature data and phase splitting, we may question the ability of the model to represent impurities, especially I_2 in the H_2SO_4 -rich phase. However, before we remove some of the assumptions related to interactions neglected interactions, we would like to obtain accuracy information on all measurements, so as to evaluate the scattering of the measurements and their true accuracy. A current study progresses in this direction.

5. Conclusion

For the first time, a model for the Bunsen section of the Sulfur – Iodine thermochemical cycle is proposed, based on UNIQUAC's activity coefficient model combined with Engels' solvation model.

Real description of all species and phenomena is discussed but is not considered because of the complexity that it brings, in particular in terms of numerous model parameters. A simpler model is proposed after noticing that water excess versus the acids, hydrogen iodide and sulfuric acid, is always greater than 3. Therefore, we postulate the total dissociation of those acids and the complete hydration of the hydronium ion by 3 water molecules. That leads to the substitution of real HI and H_2SO_4 species by apparent $[HI,3H_2O]$ and $[H_2SO_4,3H_2O]$ species. Besides, to take into account the polyiodide ions formation that is strongly suspected, $[HI,3H_2O]$ partial solvation by one I_2 molecule is described according to Engels' solvation model.

Furthermore, simplification hypotheses are proposed for the species interactions: the solvation complex of $[HI,3H_2O]$ by I_2 is supposed to interact like I_2 . and $[H_2SO_4,3H_2O]$ is supposed to interact like H_2O . Reduction of the number of parameters with temperature dependency is significant and enables to reproduce phase splitting and to launch the parameter estimation procedure.

Lee *et al.* (2008) compiled 50 Korean data as well as Sakurai *et al.* (1999, 2000) 9 data points and Giaconia *et al.* (2007) 10 data points into a comprehensive table. 45 Korean points with $n_{I_2}/n_{H_2SO_4} > 1$ are used in the estimation procedure using a relative error criterion. Other points and Kang *et al.* (2006)'s four non demixing points are used as validation.

The model reproduces all data and their demixtion with a mean relative error of 17.1% on the Korean points, below 6% for the main species (water and sulfuric acid in the H_2SO_4 rich phase; water, iodine and hydrogen iodide in the HI rich phase) and below 30% for the impurity species (iodine and hydrogen iodide in the H_2SO_4 rich phase; sulfuric acid in the HI rich phase).

For validation, Sakurai, Giaconia and kang data point are well predicted, but with larger errors than for the Korean points.

Better information on the scattering of the measurements and their true accuracy is needed to improve the model.

6. References

- [1] Funk J.E., Thermochemical hydrogen production: past and present, *Int. J. Hydrogen Energy*, 2001;26(3):185-190.
- [2] O'Keefe D., Allen C., Besenbruch G., Brown L., Norman J., Sharp R. and McCorkle K., Preliminary results from bench-scale testing of a sulfur-iodine thermochemical water-splitting cycle, *Int. J. Hydrogen Energy*, 1982;7(5):381-392.
- [3] Mathias P.M., Applied thermodynamics in chemical technology: current practice and future challenges, *Fluid Phase Equilibria*, 2005;228-229:49-57.
- [4] Hadj-Kali, M.K., Gerbaud V., Borgard J.M., Baudouin O., Floquet P., Joulia X., Carles P. HI_x System Thermodynamic model for Hydrogen Production by the Sulfur-Iodine Cycle. In press. *Int. J. Hydrogen Energy*, 2009
- [5] Brown L.C., Mathias P.M., Chen C.C., Ramrus D. Thermodynamic Model for the HI- I_2 - H_2O System, *AIChE Annual Meeting*, 4-9 November, 2001.
- [6] Mathias P.M., Brown L.C. Thermodynamics of the sulphur-iodine cycle for thermochemical hydrogen production', Presented at 68th Annual Meeting of the Society of Chemical Engineers, Japan, 2003.

- [7] Annesini M.C., Gironi F., Lanchi M., Marrelli L., Maschietti M., S-I thermochemical cycle for H₂ production: a thermodynamic analysis of the phase equilibria of the system HI-I₂-H₂O, Proceedings of ICheaP-8, The eight Italian Conference on Chemical and Process Engineering, 2007.
- [8] Roth M. and Knoche K.F., Thermo-chemical water-splitting through direct HI decomposition from HI/I₂/H₂O solutions, *Int. J. Hydrogen Energy*, 1989;14(8):545-549.
- [9] Goldstein S., Borgard J.M., Vitart X., Upper bound and best estimate of the efficiency of the iodine sulfur cycle, *Int. J. Hydrogen Energy*, 2005; 30(6):619-628.
- [10] Belaisaoui B., Thery R., Meyer X.M., Meyer M., Gerbaud V., Joulia X., Vapour reactive distillation process for hydrogen production by HI decomposition from HI-I₂-H₂O solutions, *Chem. Eng. Proc.*, 2008;47(3):396-407.
- [11] Neumann D., Phasengleichgewichte von H₂/H₂O/J₂ – Lösungen. Lehrstuhl für Thermodynamik, RWTH Aachen, 5100 Aachen (Germany). Master's thesis; January 1987.
- [12] Yoon H.J., Kim S.J., No H.C., Lee B.J., Kim E.S., A thermo-physical model for hydrogen-iodide vapor-liquid equilibrium and decomposition behavior in the iodine-sulfur thermochemical water splitting cycle, *Int. J. Hydrogen Energy*, 2008;33(20):5469-5476.
- [13] Palmer A.D., Lietzke M.H., The equilibria and kinetics of iodine hydrolysis, *Radiochimica Acta*, 1982;31:37-44.
- [14] Palmer A.D., Ramette R.W., Mesmer R.E., Triiodide ion formation equilibrium and activity coefficients in aqueous solution, *Journal of Solution Chemistry*, 1984;13(9):673-683.
- [15] Calabrese V.T., Khan A., Polyiodine and polyiodide species in an aqueous solution of iodine + KI: Theoretical and experimental studies, *J. Phys. Chem. A*, 2000;104:1287-1292.
- [16] Elder R.H., Priestman G.H., Ewan B.C., Allen R.W.K., The separation of HI_x in the sulphur – iodine thermochemical cycle for sustainable hydrogen production, *Trans IChemE, Part B*. 2005;7:343-350.
- [17] Normann J.H., Besenbuch G.E., Brown L.C., Thermo-chemical water-splitting cycle. Bench scale investigations and process engineering. DOE/ET/26225, 1981
- [18] Kracek F.C., Solubilities in the system water-iodine to 200°C, *J. Phys. Chem.*, 1931;35:417-422.
- [19] Sakurai M., Nakajima H., Rusli A, Onuki K. And Shimizu S., Experimental study on side-reaction occurrence condition in the Sulfur – Iodine thermochemical hydrogen production process', *Int. J. Hydrogen Energy*, 2000;25:613-619.
- [20] Sakurai M., Nakajima H., Onuki K., Ikenoya K., Shimizu S., Preliminary process analysis for the closed cycle operation of the iodine-sulfur thermochemical hydrogen production process, *Int. J. Hydrogen Energy*, 1999;24:603-612.
- [21] Sakurai M., Nakajima H., Onuki K. And Shimizu S., Investigation of 2 liquid phase separation characteristics on the Sulfur – Iodine thermochemical hydrogen production process, *Int. J. Hydrogen Energy*, 2000;25:605-611.
- [22] Kang Y.H., Ryu J.C., Park C.S., Hwang G.J., Lee S.H., Bae K.K., Kim Y.H., The Study on Bunsen Reaction Process for Iodine-Sulfur Thermochemical Hydrogen Production, *Korean Chem. Eng. Res.*, 2006; 44(4):410-416.
- [23] Giaconia A., Caputo G., Ceroli A., Diamanti M., Barbarossa V., Tarquini P., Sau S., Experimental study of two phase separation in the Bunsen section of the sulfur – iodine thermochemical cycle, *Int. J. Hydrogen Energy*, 2007;32:531-536.
- [24] Lee B.J., No H.C., Yoon H.J., Kim S.J., Kim E.S., An optimal operating window for the Bunsen process in the S-I thermochemical cycle, *Int. J. Hydrogen Energy*, 2008;33:2200-2210.
- [25] Davis M.E., Conger W.L., An entropy production and efficiency analysis of the Bunsen reaction in the General Atomics sulfur – iodine thermochemical hydrogen production cycle, *Int. J. Hydrogen Energy*, 1980;5, 475-485.
- [26] Mathias P.M., 2002, Modeling the sulfur-iodine cycle: Aspen Plus building blocks and simulation models, report GA and Sandia National Laboratories.
- [27] Chen C.C., Britt H.I., Boston J. F., Evans L.B., Local composition model for excess Gibbs energy of electrolyte systems. Part I: Single solvent, single completely dissociated electrolyte systems, *AIChE Journal*, 1982;28:588-596.
- [28] Chen C.C., Evans L.B., A local composition model for the excess Gibbs energy of aqueous electrolyte systems, *AIChE Journal*, 1986;32:444-454.

- [29] Pitzer K., Electrolytes. From dilute solutions to fused salts, *J. Am. Chem. Soc.*, 1980;102:2902-2906.
- [30] Renon H., Prausnitz J.M., Local compositions in thermodynamic excess functions for liquid mixtures, *AIChE Journal*, 1968;14(3):135-144.
- [31] O'Connell J., Oral Conference at ESAT (29/05/2008 – 01/06/2008), Cannes, France, 2008.
- [32] Zemaïtis J.F., D.M. Clark, R. Marshall and N.C. Scrivner, 1986, *Handbook of Aqueous Electrolyte Thermodynamics: Theory & Application*, Editions DIPPR.
- [33] Chen C.C., Mathias P.M., Orbey H., Use of hydration and dissociation chemistries with the electrolyte-NRTL model, *AIChE Journal*, 1999;45(7):1576-1586.
- [34] Anderson T.F., J.M. Prausnitz, Application of the UNIQUAC Equation to Calculation of Multicomponent Phase Equilibria. 1. Vapor-Liquid Equilibria, *Ind. Eng. Chem. Process Des. Dev.*, 1978;17 (4):552–561
- [35] Bondi A., van der Waals Volumes and Radii, *J. Phys. Chem.* 1964;68:441-451.
- [36] Abrams D.S., Prausnitz J.M., Statistical thermodynamics of liquid mixtures: A new expression for the excess Gibbs energy of partly or completely miscible systems, *AIChE Journal*, 1975;21(3):116-128.
- [37] Engels H., Phase equilibria and phase diagrams of electrolytes, *Chemistry data Series*, Volume XI, Part I. (1990) Published by DECHEMA.
- [38] Pickering S.E., Die Hydrate der Jodwasserstoffsäure 1893;2307-2310.
- [39] Zavitsas A.A., Properties of Water Solutions of Electrolytes and Nonelectrolytes, *J. Phys. Chem. B*, 2001;105:7805-7815.
- [40] ProSim, Simulis® Thermodynamics User Guide, <http://www.prosim.net>, 2004.

Table Caption

Table 1. True species binary interaction parameter matrix.

	I_2	$\{2C_3\}$	H_2O	$[H_2SO_4, 3H_2O]$	$[HI, 3H_2O]$
I_2	0		A_{12}		A_{13}
$\{2C_3\}$					
H_2O	A_{21}		0		A_{23}
$[H_2SO_4, 3H_2O]$			A_{32}		0
$[HI, 3H_2O]$	A_{31}				

Table 2. Parameters of the Bunsen section simplified model.

i	j	A_{ij}° (K)	A_{ji}° (K)	A_{ij}^T (K)	A_{ji}^T (K)
I_2	$[HI, 3H_2O]$	19.836	-387,468	0.050	0.886
I_2	H_2O	327.019	-1132.212	-1.474	6.491
I_2	$[H_2SO_4, 3H_2O]$	327.019	-1132.212	-1.474	6.491
I_2	$\{2C_3\}$	0.000	0.000	0.000	0.000
$[HI, 3H_2O]$	H_2O	-185.305	35.224	0.010	0.735
$[HI, 3H_2O]$	$[H_2SO_4, 3H_2O]$	-185.305	35.224	0.010	0.735
$[HI, 3H_2O]$	$\{2C_3\}$	-387,468	19.836	0.886	0.050
H_2O	$[H_2SO_4, 3H_2O]$	0.000	0.000	0.000	0.000
H_2O	$\{2C_3\}$	-1132.212	327.019	6.491	-1.474
$[H_2SO_4, 3H_2O]$	$\{2C_3\}$	-1132.212	327.019	6.491	-1.474
	A_K	B_K (K)			
K (eq. [24])	-1.270	850.000			

Table 3. Criterion, mean and median relative errors on experimentally measured species for the Bunsen section simplified model upon the data of Lee et al., [24]; data of Sakurai and Giaconia in Lee et al. [24].

	<i>All species</i>		<i>Impurities</i>		<i>Main species</i>	
	mean	median	mean	median	mean	median
Estimation						
<i>Lee 25°C</i>	13.5%	3.4%	30.5%	30.6%	3.3%	1.9%
<i>Lee 40°C</i>	17.1%	6.6%	32.7%	18.2%	7.7%	3.1%
<i>Lee 60°C</i>	20.0%	9.9%	41.9%	30.2%	6.9%	3.7%
<i>Lee 80°C</i>	16.0%	7.3%	31.8%	27.1%	6.5%	3.3%
<i>Lee 100°C</i>	20.5%	7.6%	45.6%	37.8%	5.5%	1.6%
<i>Lee 120°C</i>	15.9%	4.2%	33.2%	27.9%	5.6%	1.5%
<i>Lee 25 – 120°C</i>	17.1%	5.4%	27.5%	29.5%	5.8%	2.9%
Validation						
<i>Sakurai</i>	26.4%	15.7%	51.6%	55.2%	11.2%	7.4%
<i>Giaconia</i>	36.3%	14.8%	71.8%	32.8%	15.1%	12.4%

Table 4. Species mean and median relative errors on experimentally measured species for the Bunsen section simplified model upon the data of Lee et al., [24]; data of Sakurai and Giaconia in Lee et al. [24].

	<i>Upper H₂SO₄ rich phase</i>				<i>Lower HI rich phase</i>			
	I ₂ **	HI **	H ₂ O	H ₂ SO ₄	I ₂	HI	H ₂ O	H ₂ SO ₄ **
Estimation								
<i>Lee 25 – 120°C</i>								
Mean	61.0%	21.0%	1.9%	15.6%	5.2%	5.9%	2.8%	34.6%
Median	62.5%	14.7%	1.4%	9.5%	3.7%	4.9%	2.6%	27.9%
Max	94.3%	78.8%	5.5%	68.4%	21.0%	19.2%	7.1%	69.3%
Validation								
<i>Sakurai</i>								
Mean	73.9%	45.8%	2.7%	16.4%	24.1%	25.1%	10.7%	39.0%
Median	82.1%	54.5%	2.5%	15.3%	24.1%	22.1%	6.9%	41.2%
Max	94.0%	68.5%	3.7%	25.3%	33.3%	54.9%	21.3%	66.6%
<i>Giaconia</i>								
Mean	47.2%	16.4%	4.8%	28.3%	9.2%	7.2%	7.9%	68.8%
Median	48.3%	6.8%	5.8%	35.4%	9.7%	7.1%	8.4%	18.1%
Max	67.2%	42.3%	7.8%	44.5%	17.2%	14.7%	11.0%	494.1%

Figure 1. Sulfur – Iodine thermo-chemical cycle scheme [1].

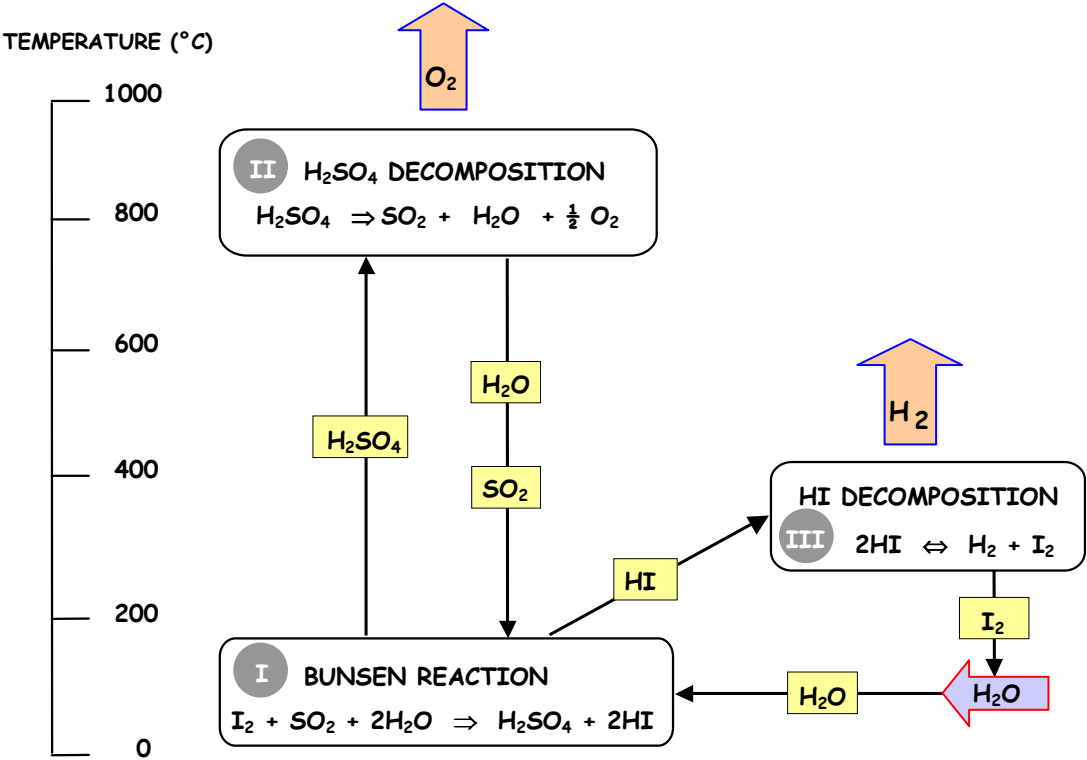


Figure 2. Comparison of experimental and calculated values for Korean data points at 25°C and 40°C reported in Lee et al. [24].

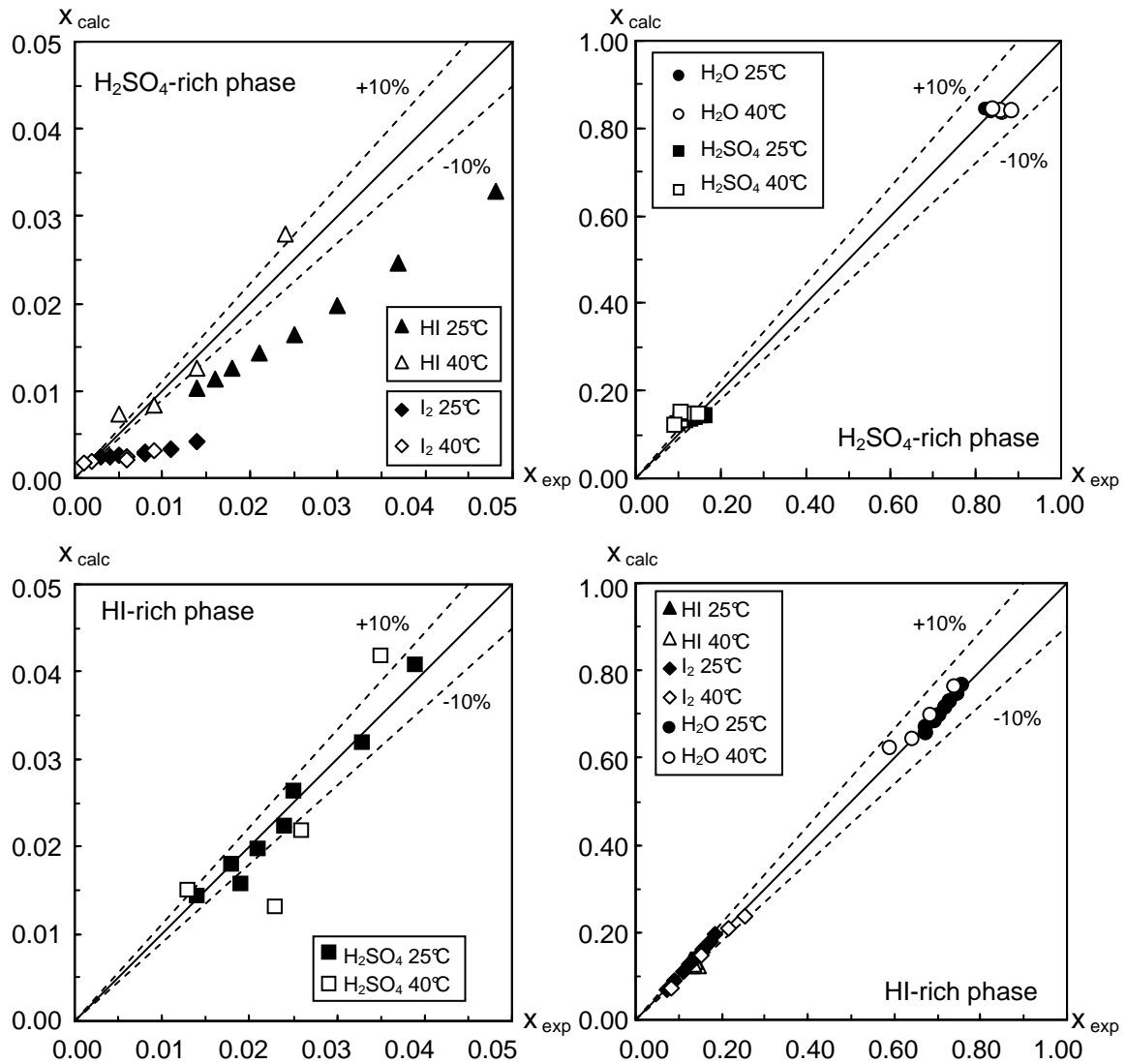


Figure 3. Comparison of experimental and calculated values for Korean data points at 60°C and 80°C reported in Lee et al. [24].

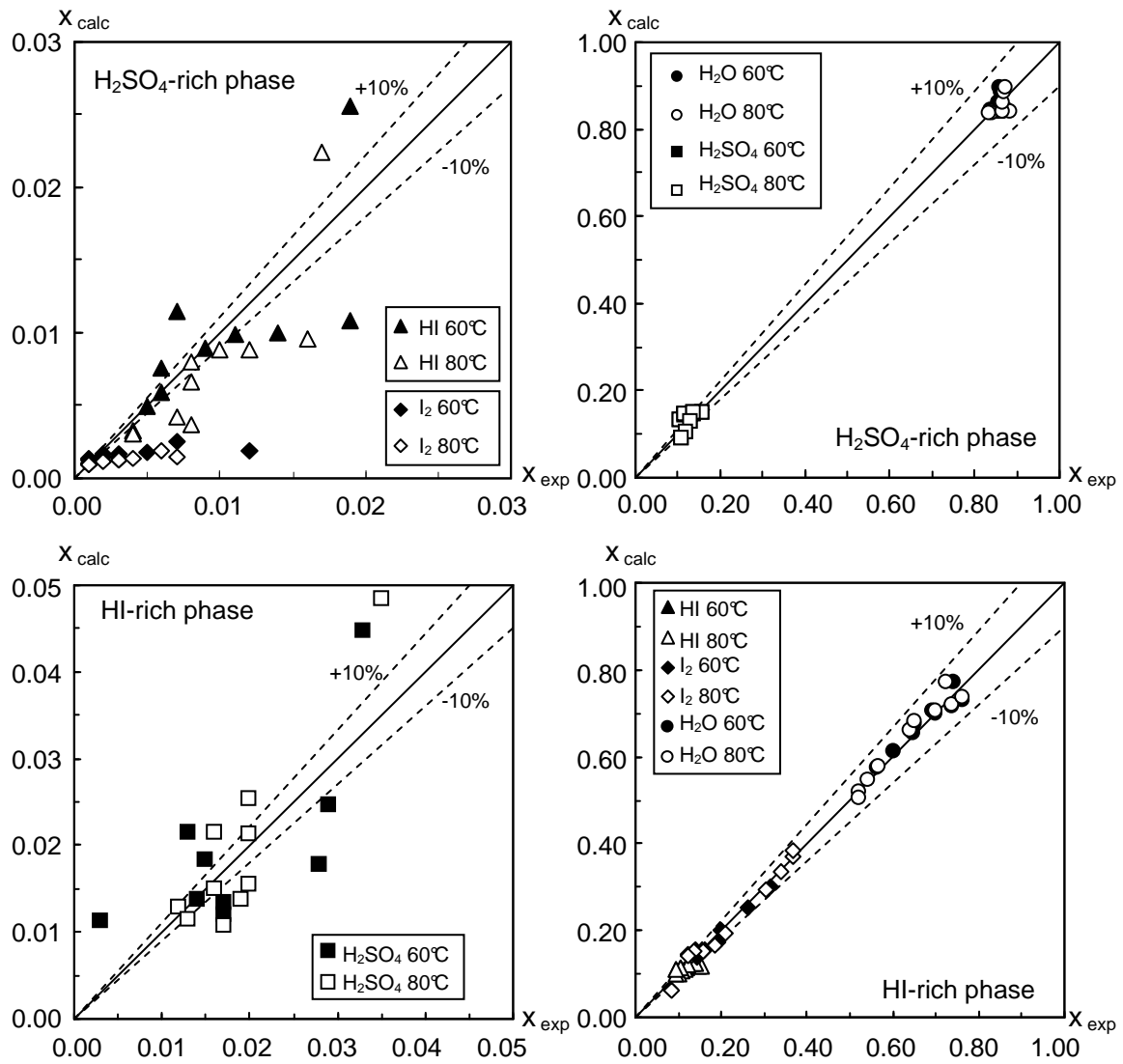


Figure 4. Comparison of experimental and calculated values for Korean data points at 100°C and 120°C reported in Lee et al. [24].

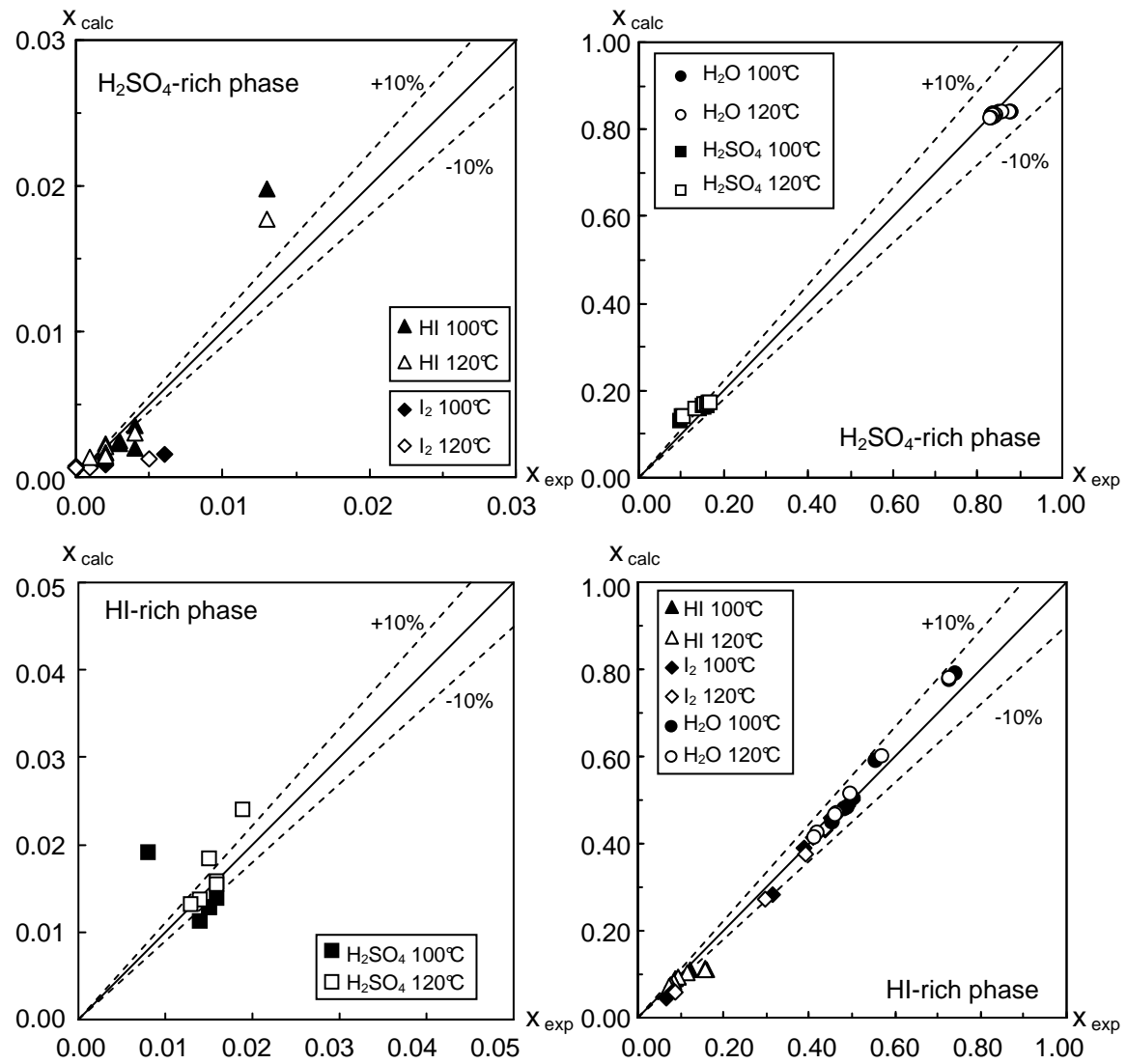


Figure 5. Comparison of experimental and calculated values for data points of Sakurai (S01-S09) and Giaconia (G01-G10) reported in Lee et al. [24].

